Journal of Applied Science and Engineering, Vol. 17, No. 2, pp. 141−156 (2014) *DOI: 10.6180/jase.2014.17.2.05*

Vibration Control in a 101-Storey Building Using a Tuned Mass Damper

Alex Y. Tuan[1]* and G. Q. Shang[2]

[1]*Department of Civil Engineering, Tamkang University, Tamsui, Taiwan 251, R.O.C.*
[2]*Department of Civil and Architectural Engineering, City University of Hong Kong, Hong Kong*

Abstract

This study investigates the mitigating effects of a TMD on the structural dynamic responses of Taipei 101 Tower, under the action of winds and remote (long-distance) seismic excitation. To begin with, the optimal parameters of the TMD in Taipei 101 Tower are first determined. Then a finite element model of this high-rise building, equipped with a TMD system, is established. A detailed dynamic analysis is conducted accordingly, to evaluate the behavior of the structure-TMD system. The simulation results obtained are compared with the wind tunnel test data and the recorded field measurements. The accuracy of the established computational frameworks is then verified. Findings of this study demonstrate that the use of the TMD in this building is materially effective in reducing the wind-induced vibrations. However, it is not as effective in mitigating remote seismic vibrations responses.

Key Words: Vibration Control, Tuned Mass Damper (TMD), Structure-TMD Interaction, Dynamic Analysis, Wind Effect, Earthquake Excitation, FEM, Wind Tunnel Testing, Field Measurement

1. Introduction

Advances in new materials, the progress in new structural systems, as well as the developments in computational software and design methods, have made possible the construction of extremely tall buildings in modern days. However, the ever-increasing height of the high-rise structure poses considerable challenges for structural engineers and researchers in this field. Among the many difficult technical problems involved in design, the effects of wind and earthquakes on these structures are definitely the most critical issues.

The most important task to be overcome is, both the criteria of serviceability and safety (strength) must be carefully considered and satisfied in the design. For modern buildings become taller, they also become more flexible and slender. Such structures are almost always sensitive to wind excitations, and therefore serviceability becomes a critical issue. Under most circumstances, the inherent damping in a tall building itself is not sufficient to satisfy the serviceability requirements. In addition, it has been shown [1,2] that remote earthquakes are able to generate base shears up to a magnitude comparable to that of the notional horizontal load, which is sometimes even greater than the wind loading. In particular, high-rise buildings can be very sensitive to dynamic excitations by remote(long-period) earthquakes [3]. Therefore, in order to reduce the dynamic responses of high-rise structures to meet the serviceability criterion [4], many strategies are considered in terms of increasing the structural damping to achieve the goal. Basically, these methods can be roughly divided into two categories: passive control and active control strategies. As reported in many successful implementations, the wind-induced st-

*Corresponding author. E-mail: alextuan@mail.tku.edu.tw

ructural responses can be substantially reduced by using passive control methods, such as the incorporation of auxiliary damping systems: viscoelastic dampers, damping walls, and TMD (tuned mass damper) or TLD (tuned liquid damper) [5], etc.

A tuned mass damper (TMD) is a large, massive block, which is usually mounted on the top or near the top of a tall building. The system consists of a mass, springs and damping devices. Its frequency can be tuned to match the predominant vibration frequency (usually the first modal frequency) of the main structure. So that the structural dynamic responses caused by environmental excitations, such as strong winds and earthquakes, can be significantly reduced. The 508-m tall Taipei 101 Tower is a primary example, which has the world's largest TMD (660 tons) system for the control of structural vibrations.

TMD was first suggested by Frahm in 1909, to attenuate undesirable vibrations in ships. The device consists of a mass (m), springs (k) and damping devices (c). While attached to the main system, the dynamic behavior of that system can be altered. Up to now, TMDs have been successfully installed in many civil engineering structures to control the structural vibrations due to environmental disturbances. Especially in many skyscrapers and slender towers worldwide. Namely, the CN Tower (535 m) in Canada, the John Hancock Building (60 stories) in Boston, USA, Center-Point Tower (305 m) in Sydney, Australia, and the once tallest building in the world – Taipei 101 Tower (101 stories, 508 m), in Taipei. Recently, many studies have been focused on finding the optimum parameters for TMDs and on evaluating its efficiency under various type of dynamic excitations. For minimize the displacement of a single-degree-of-freedom (SDOF) main structure, Den Hartog [6] derived classic results for the optimum TMD parameters for harmonic external forces. Using similar conditions, Chang [7] obtained the optimum parameters for a TMD under broadband white noise excitation. Sgobba and Marano [8] examined the optimum design parameters for a TMD for the seismic protection of inelastic structures. However, when the damping of the main structure is included, the closed-form analytical expressions for the optimal parameters of a TMD have not been derived. Leung [9, 10] used particle swarm optimization (PSO) to described the optimal numerical parameters for a TMD for different external excitations to the main structural system, such as harmonic-based acceleration, white-noise-based acceleration and non-stationary-based acceleration. Lee et al. [11] extended the optimal design theory for a TMD to a multiple-degrees-of-freedom (MDOF) structure, with multiple TMDs (MTMDs) installed on different floors, to address the environmental disturbances generated by the power spectral density (PSD) function. Xu et al. [12] and Gerges and Vickery [13] conducted wind tunnel tests to study the structural dynamic behavior of super tall buildings with TMD system. Rana and Soong [14] performed a parametric study and produced a simplified design procedure for a TMD. It is shown in the study, compared with realistic excitations, using harmonic excitations in the TMD design can give reasonable results as well. However, to the best knowledge of the authors, there are no studies of the effectiveness of TMD's in real super tall buildings and neither of the performance of controlled super tall buildings under the action of a typhoon or an earthquake. Obviously, proper modeling of the TMD-structure interaction is required in the design of TMD-controlled structures. Nevertheless, this type of study for super tall buildings is hardly found. Analytical models for the structural analysis of high-rise buildings rarely take into account the installed TMD apparatus. Actually, these models usually consider the effect of a TMD by only elevating damping ratio values, which is insufficient to reflect the nature of the structure-control interaction and the realistic dynamic behaviors of systems.

This paper uses an analogy between a SDOF system and a MDOF system, both with a TMD, to produce an optimal design for the TMD – structure system. By minimizing the acceleration of the controlled main structure and by considering the serviceability criteria, the optimal parameters for the TMD system equipped in the Taipei 101 Tower are derived. The classic parameter optimism theory is used. Then, in the computational framework, a 3D-FEM model of this super tall building is established by ANSYS 12.0. With the emphasis on incorporate the TMD into the main structural system and properly model the structure-control device interaction. Utilized the wind flow generated by computational fluids dynamics (CFD) as the wind loads subjected on the structure, the wind-induced vibration responses of this tall building

structure, controlled by a TMD, are analyzed and computed. Compared to the available wind tunnel test data and the recorded field measurements, the computational results encouragingly show that the wind-induced responses of this super tall building can be substantially reduced. The mitigating effect of the TMD system on remote (long-period) seismic-induced vibrations in the Taipei 101 Tower is also analyzed. The results show that the mitigation effect due to the long-distance seismic excitation is not as good as that due to the wind action. This may be attributable to the different excitation mechanisms for winds and earthquakes, which cause different effects on tall building structure. The results of this comprehensive study are believed to be very significant and useful for engineers and researchers, who are practicing in design of super tall buildings incorporated with TMD systems.

2. Methodology

2.1 The Parameter Optimization Theory for a TMD

Over the last several decades, the parameter optimization theory for TMD's has been the subject of considerable research interest. Intensive studies have been conducted to determine the optimal parameters for a TMD under various excitations, to calculate the responses of the main structures, and to evaluate the efficiency of the TMD contributions in terms of mitigating vibration in the main structures. Warburton and his collaborators [15–17] performed systematical studies to determine the optimal parameters for a TMD. They derived the closed form expressions for the optimal parameters of an absorber, as well as for system responses. The system considered in their studies consisted of an undamped SDOF main system and an attached TMD, which was subjected to steady-state harmonic excitations and random excitations with white noise spectral density. They also extended the formulae to an elastic body without damping and one with light damping. These studies demonstrated that an elastic body can be replaced by an equivalent SDOF system, for the purpose of determining the optimal parameters of its attached TMD. Provided that the frequencies of the elastic body are well separated, and the dynamic response is majorly contributed by the fundamental mode. The results concluded that in order to minimize the fundamental resonance of an elastic body, a TMD with a small mass ratio between the absorber system and the main system is preferable. As long as the natural frequencies satisfy the condition, $\omega_1/\omega_2 \le 0.5$ (where ω_1 and ω_2 represent the first and second fundamental frequencies of the elastic body, respectively), the equivalent system yields the optimal parameters for the TMD. And the associated structural responses are minimized into an acceptable range of accuracy. As for the damping of the main system, it is suggested that limited damping of the main system has very little effect on the TMD's optimal parameters. For real systems with light damping, if this frequency condition is satisfied, it is reasonable to use the optimal parameters of the TMD for the undamped equivalent system to minimize the dynamic response of the system.

The equations for a TMD attached to an undamped SDOF system, as shown in Figure 1, are:

$$M_m\ddot{x} + K_m x + c_a\dot{x} + k_a x - c_a\dot{x}_a - k_a x_a = p(t) \tag{1}$$

$$m_a\ddot{x}_a + c_a\dot{x}_a + k_a x_a - c_a\dot{x} - k_a x = 0 \tag{2}$$

where M_m, K_m, and x are the mass, stiffness, and displacement of the system, respectively; while m_a, c_a, k_a, and x_a are the mass, damping, stiffness, and displacement of the TMD, respectively. In the case of a harmonic force acting on the system, $p(t) = pe^{i\omega t}$, the displacement, velocity and acceleration of the main system are expressed as:

$$x = \frac{(k_a - m_a\omega^2 + i\omega c_a)pe^{i\omega t}}{(K_m + k_a - M_m\omega^2 + i\omega c_a)(k_a - m_a\omega^2 + i\omega c_a) - (k_a + i\omega c_a)^2} \tag{3}$$

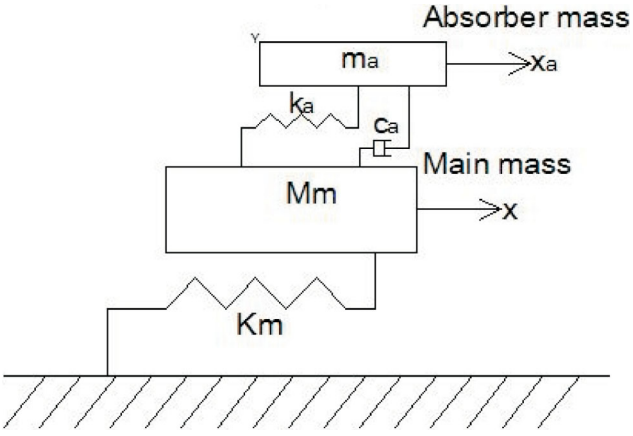

Figure 1. A SDOF-TMD system.

$$\dot{x} = \frac{(k_a - m_a\omega^2 + i\omega c_a)i\omega p e^{i\omega t}}{(K_m + k_a - M_m\omega^2 + i\omega c_a)(k_a - m_a\omega^2 + i\omega c_a) - (k_a + i\omega c_a)^2} \quad (4)$$

$$\ddot{x} = \frac{-\omega^2(k_a - m_a\omega^2 + i\omega c_a)p e^{i\omega t}}{(K_m + k_a - M_m\omega^2 + i\omega c_a)(k_a - m_a\omega^2 + i\omega c_a) - (k_a + i\omega c_a)^2} \quad (5)$$

where the following parameters are introduced:
Mass ratio: $\mu = m_a/M_m$
Tuning ratio: $f = \omega_a/\omega_m$
$\omega_a^2 = k_a/m_a$, $\omega_m^2 = k_m/M_m$
Forced frequency ratio: $r = \omega/\omega_m$
Absorber damping ratio: $\gamma_a = c_a/2m_a\omega_a$,
the dimensionless forms of the main system's displacement, velocity and acceleration responses can be expressed as follows:

$$x = \frac{(f^2 - r^2 + 2ir\gamma_a f)}{(\mu f^2 - r^2 + 1 + 2i\mu r\gamma_a f)(f^2 - r^2 + 2ir\gamma_a f) - \mu(f^2 + 2i\gamma_a fr)^2} \cdot \frac{p e^{ir\omega_m t}}{K_m} \quad (6)$$

$$\dot{x} = \frac{(f^2 - r^2 + 2ir\gamma_a f)}{(\mu f^2 - r^2 + 1 + 2i\mu r\gamma_a f)(f^2 - r^2 + 2ir\gamma_a f) - \mu(f^2 + 2ir\gamma_a f)^2} \cdot \frac{pir\omega_m e^{ir\omega_m t}}{K_m} \quad (7)$$

$$\ddot{x} = \frac{(f^2 - r^2 + 2ir\gamma_a f)}{(\mu f^2 - r^2 + 1 + 2i\mu r\gamma_a f)(f^2 - r^2 + 2ir\gamma_a f) - \mu(f^2 + 2ir\gamma_a f)^2} \cdot \frac{-pr^2\omega_m^2 e^{ir\omega_m t}}{K_m} \quad (8)$$

The optimal parameters for the TMD are shown in Table 1. The design parameters for the TMD are:

$$k_a = m_a\omega_m^2 f_{(opt)}^2$$
$$c_a = 2\gamma_{a(opt)} m_a (k_a / m_a)^{1/2} \quad (9)$$

For the MDOF system shown in Figure 2, the equations of the combined system are expressed as:

$$M\ddot{X} + KX + c_a\dot{X}' + k_a X' - c_a\dot{Y} - k_a Y = Pe^{i\omega t} \quad (10)$$

$$m_a\ddot{Y} + c_a\dot{Y} + k_a Y - c_a\dot{X}' - k_a X' = 0 \quad (11)$$

where K and M are symmetric stiffness and mass matrices, respectively, X is the displacement vector of the main system and $X' = (0, 0, \ldots, X_j, \ldots, 0, 0)^T$ represents the displacement of M_j of the main system where a TMD is installed. Similarly, $Y = (0, 0, \ldots, x_a, \ldots, 0, 0)^T$ represents the displacement of the TMD attached to the main system. If the excitation is a vector of a harmonic force, namely $P(t) = Pe^{i\omega t}$, is applied in the direction of X, Z is the matrix of the orthogonal characteristic modes of the system and z_r is the vector of the *rth* mode, $Z_r = (Z_{1r}, Z_{2r}, \ldots, Z_{jr}, \ldots, Z_{nr})^T$.

Table 1. The optimal parameters for a TMD attached to a SDOF system

Minimizing items	$f_{(opt)}^2$	$\gamma_{a(opt)}^2$
X	$\frac{1}{(1+\mu)^2}$	$\frac{3\mu}{8(1+\mu)^3}$
$\dot{X}$	$\frac{1+0.5\mu}{(1+\mu)^2}$	$\frac{\mu(3+3\mu+0.625\mu^2}{4(2+\mu)(1+\mu)^3}$
$\ddot{X}$	$\frac{1}{(1+\mu)}$	$\frac{3\mu}{4(2+\mu)(1+\mu)}$

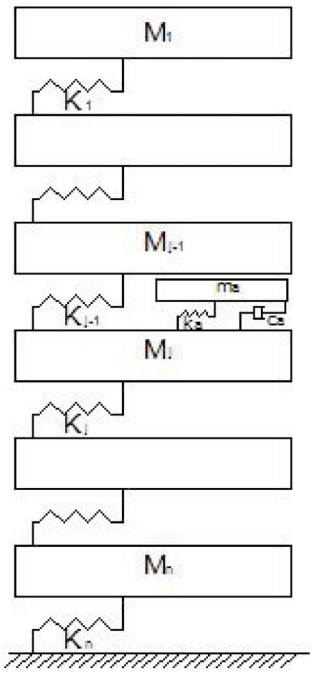

Figure 2. A MDOF-TMD system.

therefore

$$Z_r^T M Z_r = M_r \tag{12}$$

where M_r is the rth modal mass,

$$Z_r^T K Z_r = K_r = M_r \omega_r^2 \tag{13}$$

in which ω_r is the natural circular frequency of the *rth* mode. Introducing the relationship, $X = Z_r \eta_r$, and replacing the displacement of the main system, X, with the general coordinate, η_r, and pre-multiplying Z_r^T to both sides of equations (10) and (11), gives:

$$\begin{aligned} &Z_r^T M Z_r \ddot{\eta}_r + Z_r^T K Z_r X + c_a Z_r^T \dot{X}' + k_a Z_r^T X' \\ &- c_a Z_r^T \dot{Y} - k_a Z_r^T Y = Z_r^T P e^{i\omega t} \end{aligned} \tag{14}$$

$$m_a Z_r^T \ddot{Y} + c_a Z_r^T \dot{Y} + k_a Z_r^T Y - c_a Z_r^T \dot{X}' - k_a Z_r^T X' = 0 \tag{15}$$

These equations can be simplified as:

$$\begin{aligned} &M_r \ddot{\eta}_r + K_r X + c_a Z_{jr} \dot{X}_j + k_a Z_{jr} X_j - c_a Z_{jr} \dot{x}_a - k_a Z_{jr} x_a \\ &= \sum_{j=1}^{n} Z_{jr} P_j e^{i\omega t} \end{aligned} \tag{16}$$

$$m_a Z_{jr} \ddot{x}_a + c_a Z_{jr} \dot{x}_a + k_a Z_{jr} x_a - c_a Z_{jr} \dot{X}_j - k_a Z_{jr} X_j = 0 \tag{17}$$

If the relationship, $X_j = \sum_{r=1}^{n} Z_{jr} \eta_r$, is used for X_j, these equations are coupled. Since a TMD is used to mitigate the resonant response of M_j, associated with the *rth* mode, it can be assumed that the response of M_j, where the TMD is attached, makes the major contribution to the rth mode [17], so:

$$X_j \approx Z_{jr} \eta_r \tag{18}$$

Substituting equation (18) into equations (16) and (17) and solving the resulting simultaneous equations gives:

$$\eta_r = \frac{(k_a - m_a\omega^2 + i\omega c_a)\sum_{j=1}^{n} Z_{jr} P_j e^{i\omega t}}{(K_r - M_r\omega^2 + Z_{rj}^2 k_a + Z_{rj}^2 i\omega c_a)(k_a - m_a\omega^2 + i\omega c_a) - Z_{rj}^2 (k_a + i\omega c_a)^2} \tag{19}$$

If it is defined that $M_{eff} = M_r / Z_{rj}^2$, $K_{eff} = K_r / Z_{rj}^2$, so

$$\eta_r = \frac{\sum_{j=1}^{n} Z_{jr} P_j e^{i\omega t}}{Z_{jr}^2} \cdot \frac{(k_a - m_a\omega^2 + i\omega c_a)}{(K_{eff} - M_{eff}\omega^2 + k_a + i\omega c_a)(k_a - m_a\omega^2 + i\omega c_a) - (k_a + i\omega c_a)^2} \tag{20}$$

The displacement, velocity and acceleration of the mass M_s are

$$X_s = \sum_{s=1}^{n} Z_{sr} \eta_r = \sum_{s=1}^{n} Z_{sr} \left(\frac{\sum_{j=1}^{n} Z_{jr} P_j e^{i\omega t}}{Z_{jr}^2} \right) \frac{(k_a - m_a\omega^2 + i\omega c_a)}{(K_{eff} - M_{eff}\omega^2 + k_a + i\omega c_a)(k_a - m_a\omega^2 + i\omega c_a) - (k_a + i\omega c_a)^2} \tag{21}$$

$$\dot{X}_s = \sum_{i=1}^{n} Z_{sr} \dot{\eta}_r = \sum_{s=1}^{n} Z_{sr} \left(\frac{\sum_{j=1}^{n} Z_{jr} P_j e^{i\omega t}}{Z_{jr}^2} \right) \frac{i\omega(k_a - m_a\omega^2 + i\omega c_a)}{(K_{eff} - M_{eff}\omega^2 + k_a + i\omega c_a)(k_a - m_a\omega^2 + i\omega c_a) - (k_a + i\omega c_a)^2} \tag{22}$$

$$\ddot{X}_s = \sum_{s=1}^{n} Z_{sr} \ddot{\eta}_r = \sum_{s=1}^{n} Z_{sr} \left(\frac{\sum_{j=1}^{n} Z_{jr} P_j e^{i\omega t}}{Z_{jr}^2} \right) \frac{-\omega^2(k_a - m_a\omega^2 + i\omega c_a)}{(K_{eff} - M_{eff}\omega^2 + k_a + i\omega c_a)(k_a - m_a\omega^2 + i\omega c_a) - (k_a + i\omega c_a)^2} \tag{23}$$

For a MDOF system, similar parameters can be introduced: $\mu = m_a / M_{eff}$, $\omega_a^2 = k_a / m_a$, $\omega_r^2 = k_{eff} / M_r$, $f = \omega_a / \omega_r$, $r = \omega / \omega_r$, $\gamma_a = c_a / 2 m_a \omega_a$.

The dimensionless forms of X_s, $\dot{X}_s$ and $\ddot{X}_s$ can be expressed as:

$$X_s = \sum_{s=1}^{n} Z_{rs} \left(\frac{\sum_{j=1}^{n} Z_{jr} P_j e^{i\omega t}}{K_r} \right) \frac{(f^2 - r^2 + 2ir\gamma_a f)}{(\mu f^2 - r^2 + 1 + 2i\mu r\gamma_a f)(f^2 - r^2 + 2ir\gamma_a f) - \mu(f^2 + 2i\gamma_a f r)^2} \tag{24}$$

$$\dot{X}_s = \sum_{s=1}^{n} Z_{sr} \left(\frac{\sum_{j=1}^{n} Z_{jr} P_j e^{i\omega t}}{K_r} \right) \frac{i\omega(f^2 - r^2 + 2ir\gamma_a f)}{(\mu f^2 - r^2 + 1 + 2i\mu r\gamma_a f)(f^2 - r^2 + 2ir\gamma_a f) - \mu(f^2 + 2i\gamma_a fr)^2} \quad (25)$$

$$\ddot{X}_s = \sum_{s=1}^{n} Z_{sr} \left(\frac{\sum_{j=1}^{n} Z_{jr} P_j e^{i\omega t}}{K_r} \right) \frac{-\omega^2(f^2 - r^2 + 2ir\gamma_a f)}{(\mu f^2 - r^2 + 1 + 2i\mu r\gamma_a f)(f^2 - r^2 + 2ir\gamma_a f) - \mu(f^2 + 2i\gamma_a fr)^2} \quad (26)$$

The optimal parameters are obtained using these equations. As an analogy with a SDOF system, when the equation, $\mu = m_a/M_{eff}$, is used and the frequency of the MDOF system is well separated. With $\omega_1/\omega_2 \le 0.5$, the optimal parameters of a TMD installed in a MDOF system are obtained, as shown in Table 2. The design parameters necessary for the TMD to reduce the vibration of the rth mode are expressed as:

$$k_a = m_a \omega_r^{\ 2} f_{(opt)}^{\ 2}$$
$$c_a = 2\gamma_{a(opt)} m_a (k_a / m_a)^{1/2} \quad (27)$$

3. An Introduction of the Taipei 101 Tower and Its TMD System

Taipei 101 Tower, as shown in Figure 3, is located in Hsinyi District in Taipei. This super tall structure is a 101-storey office building with five levels of basements, from -19.4 m below ground level to 508 m above ground. It was the tallest building in the world when it was built eleven years (2002) ago. A 660 ton TMD is installed on an upper floor of the building, as shown in Figure 4(a), to reduce its dynamic responses to winds and earthquakes and to meet the requirement for comfortable habitation. Field measurements and numerical analysis of the dynamic behaviors of this building has been investigated thoroughly by Li et al. [3].

As shown in Figure 4 (a), the major part of the TMD system is a 6 m-diameter sphere that is made of steel and weighs 660 tons. It is the largest of its kind in the world. It is installed at the center of the 87th floor and suspended from the 91st floor by cables. There are eight dampers around the mass, to prevent it from moving excessively. This TMD is essentially a pendulum that spans five floors (88th~92th), whose primary function is to suppress wind-induced vibrations in this building. It is also de-

Table 2. The optimal parameters for a TMD attached to a MDOF system

Minimizing items	$f_{(opt)}^{\ 2}$	$\gamma_{a(opt)}^{\ 2}$
X	$\frac{1}{(1+\mu)^2}$	$\frac{3\mu}{8(1+\mu)^3}$
$\dot{X}$	$\frac{1+0.5\mu}{(1+\mu)^2}$	$\frac{\mu(3+3\mu+0.625\mu^2}{4(2+\mu)(1+\mu)^3}$
$\ddot{X}$	$\frac{1}{(1+\mu)}$	$\frac{3\mu}{4(2+\mu)(1+\mu)}$

Note: $\mu = m_a/M_{eff}$, $f = \omega_a/\omega_r$, $\gamma_a = c_a/2m_a\omega_a$.

Figure 3. Photo of Taipei 101 Tower.

signed to withstand the forces generated in a strong seismic event, with a return period of 2500 years [18]. Taking into account the character of the vibration in a typical high-rise building under the action of wind, the fundamental mode usually governs the structural dynamic responses, so the most effective way to reduce wind-induced dynamic responses is to mitigate the fundamental modal response of the structure. As Taipei 101 Tower is symmetrical, there are two fundamental modals, in the X and Y directions. Since the fundamental modal responses can be mitigated in the two directions simultaneously by the pendulum and the amplitude of the pendulum is relatively small, the system is able to be simplified as two horizontally orthogonal spring oscillators, as shown in Figure 4 (b). Furthermore, the interaction between the TMD and the structure can be assumed to be independent in the direction of X and Y, because of the nature of modal orthogonality. The model shown in Figure 4(b) can be further simplified as two independent TMDs. For each TMD, the optimal parameter theory as previously discussed, can be used to determine its optimal parameters in both the X and Y directions.

4. A Numerical Analysis of the Combined System of the Taipei 101 Tower and the TMD

It is well known that high-rise structures will experience along-wind vibration and across-wind vibration, as well as a torsional response. The former is due to the buffeting induced by fluctuations in the wind velocity and the across-wind force, and the responses are mainly governed by vortex shedding. For slender structures, the across-wind vibration is usually more severe than the along-wind vibration. Therefore, in most cases, it is the major factor in wind-induced vibration in a high-rise buildings such as the Taipei 101 Tower. However, the displacement and acceleration near the peripheries of the building may be increased due to the wind-induced torsional vibrations. Unfortunately, the nature of the across-wind and torsional vibrations are extremely complex that, despite extensive studies, the mechanisms of such vibrations have not been able to described sufficiently. Therefore, no general analytical methods are available to accurately calculate these responses. A more practical method for evaluating the efficiency of a TMD's dissipation

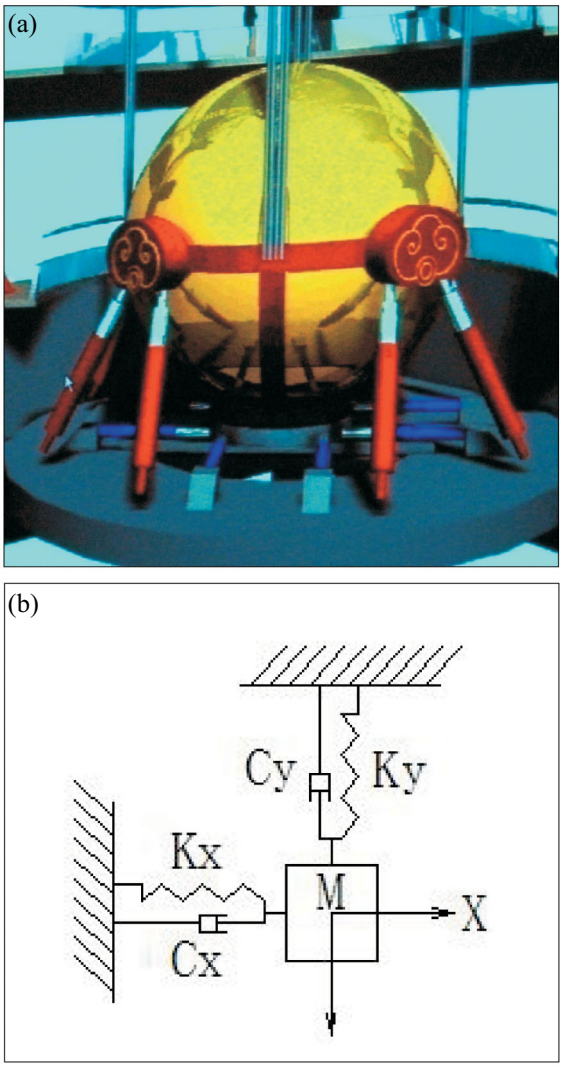

Figure 4. (a) The TMD installed in Taipei 101 Tower. (b) Mechanical model of the TMD in Taipei 101 Tower.

of the dynamic responses is to use a simplified representation of the wind action as a harmonic load, assuming that the most unfavorable value is in the vicinity of one of the natural frequencies of the structure. In general, the fundamental frequency is chosen [19]. Results of the wind tunnel test for Taipei 101 Tower [20] predicted that the across-wind response dominates the overall wind-induced vibration. Therefore the simulation scheme for the dynamic responses of the Taipei 101 Tower (with TMD) can be summarized as follows:

Step 1: A modal analysis of the Taipei 101 Tower without TMD system is first conducted, in order to find the fundamental vibration modes to be mitigated.

Step 2: The optimal parameter theory is then utilized to find the optimal parameters for this TMD system. The objective is to minimize the acceleration of the upper floors of this super tall building.

Step 3: The wind tunnel test results and/or the CFD simulation results are then used to determine the wind loads subject on the building. For earthquake excitations, the records measured on the building site are used as the inputs for seismic analysis of this structure.

Step 4: Eventually, a dynamic analysis of the combined system of the Taipei 101 Tower with the TMD is conducted, to evaluate the effectiveness of the TMD in reducing the vibrations of the building, while it is subjected to wind loads or seismic forces.

5. The 3D-FEM Model Incorporating the TMD

Based on the design drawings, a detailed 3D-FEM model of Taipei 101 Tower is established by using ANSYS 12.0. The FEM model uses beam elements, shell elements, link elements and mass elements to model the structural system of the Taipei 101 Tower and the TMD. The amplitude-dependent damping character of the TMD is considered as equivalent viscous damping. The TMD system is modeled using two spring systems in both X and Y directions, located at the centroid of the 88th floor. Constrain equations are also used to combine the TMD system with the Taipei 101 Tower. The wind loads on the tall building are determined by a large eddy simulation (LES) [21] and typical examples of the simulated wind forces are shown in Figure 5. The earthquake record, measured at the lowest floor of the basement in the Taipei 101 Tower during the Wen Chuan earthquake [3], are used to the 3D-FEM model incorporating with the TMD, for dynamic analysis. The completed model is illustrated in Figure 6 (a) and (b).

6. Results and Discussions

6.1 Modal Analysis

As an effective passive control device, the major contribution of the TMD is to reduce the dynamic responses of the structure by altering the fundamental frequency (first mode) of the structure, so that the acceleration of the top residential floors can be controlled to satisfy the safety criterion as well as the serviceability criterion for human comfort. In order to achieve this goal, the optimal parameters of the TMD were derived, as shown in Table 3. It is also listed in Table 4 the results from equation (27) and the natural frequencies of the building (with and without TMD).

The modal analysis results are shown in Figures 7–8 and Table 4. Due to the symmetry feature of the building, the first two frequencies are identical. As the TMD is installed, the first mode in the X and Y directions becomes two modes. This situation is similar to the SDOF system. Which is the expected way that the TMD is to perform. The modification of the modes therefore suppresses the

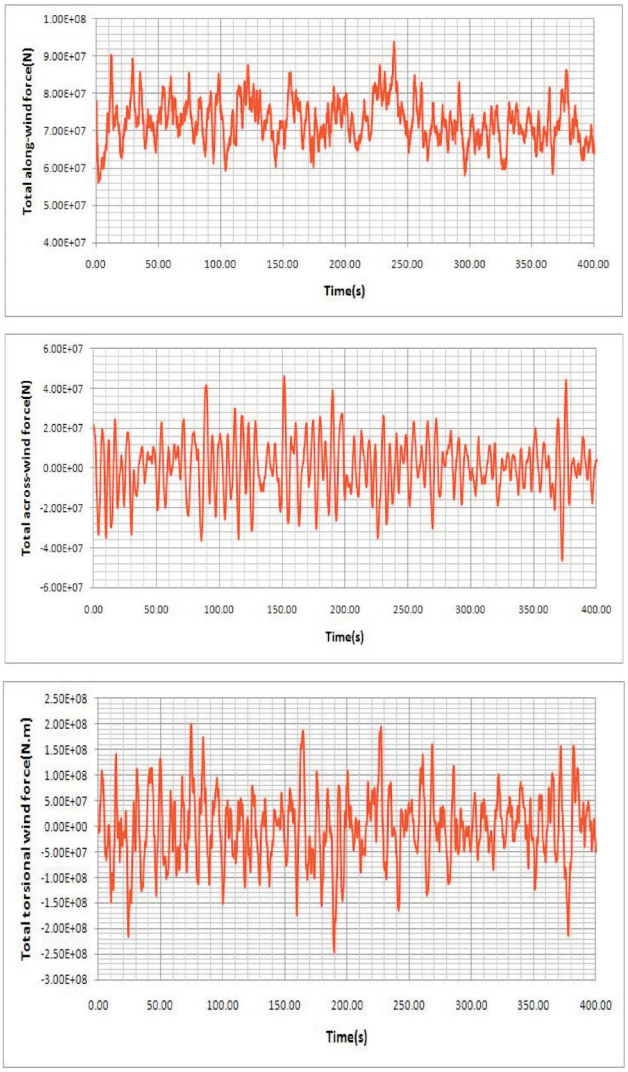

Figure 5. Time histories of the total force F_L, F_D, M.

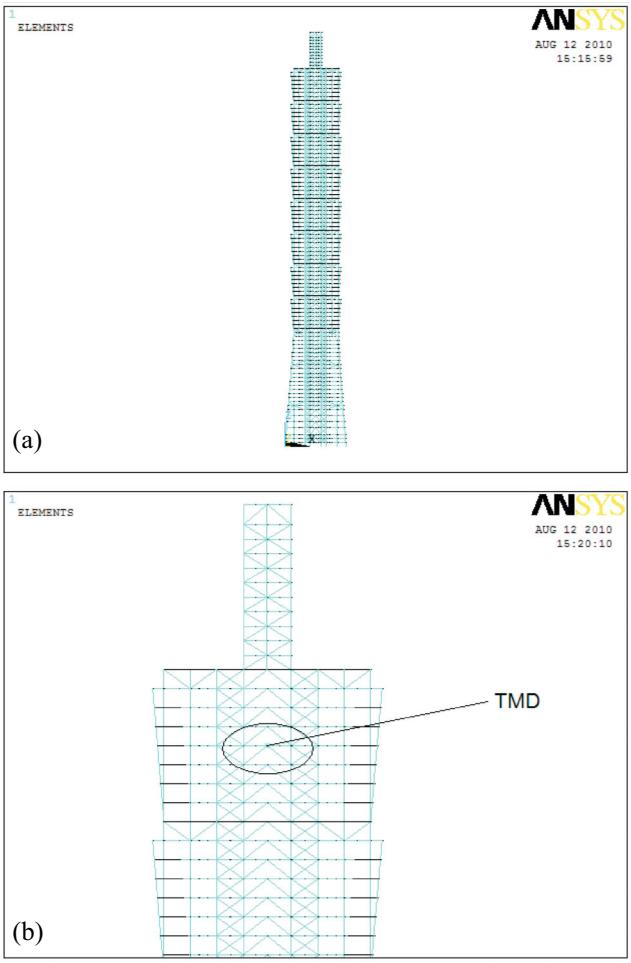

Figure 6. (a) FEM model of Taipei 101 Tower. (b) FEM model of Taipei 101 Tower with the TMD.

Table 3. The optimal parameters for the TMD installed in the Taipei 101 Tower

M_{eff} (T)	m_a (T)	μ	k_a (kN/m)	γ_a
39655	660	0.0166	1118807	0.037

Note: $k_a = m_a\omega_1^2 f_{(opt)}^2$, $\gamma_a = c_a/2m_a\omega_a$

dynamic responses of the high-rise structure accordingly.

7. Wind-Induced Vibration Effectively Controlled by the TMD System

It is observed that, as in Table 5, Figures 9(a) and 10(a), while the TMD system is installed, the along-wind and across-wind displacements on the uppermost occupied floor (89th floor) are reduced significantly. The benefit can also be expected on the improvement of the long-term building performance. Since the durability of those nonstructural components, such as the claddings,

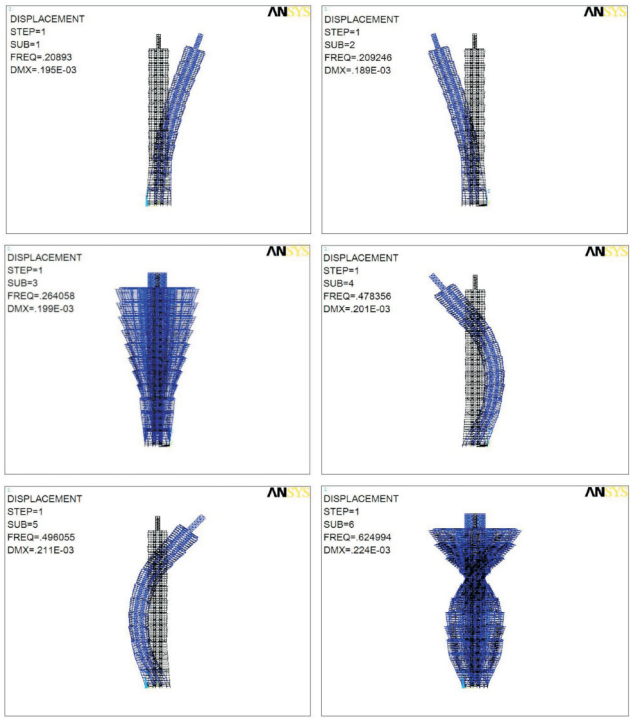

Figure 7. Several mode shapes of Taipei 101 Tower without TMD.

Table 4. The natural frequencies of the Taipei 101 Tower

Modal frequency (Hz)	The first mode in the X direction		The first mode in the Y direction		The first mode of the rotational direction	The second mode in the X direction	The second mode in the Y direction	The second mode of the rotational direction
Without TMD	0.2092		0.2089		0.264	0.478	0.496	0.625
With TMD	0.173	0.222	0.173	0.222	0.264	0.479	0.497	0.625
Full-scale measurement	0.146	--	0.152	--	0.242	0.435	0.428	--
Difference (%)	18.5	--	13.8	--	9.1	--	--	--

Note: *difference* = (*calculated* – *measured*)/*measured*.

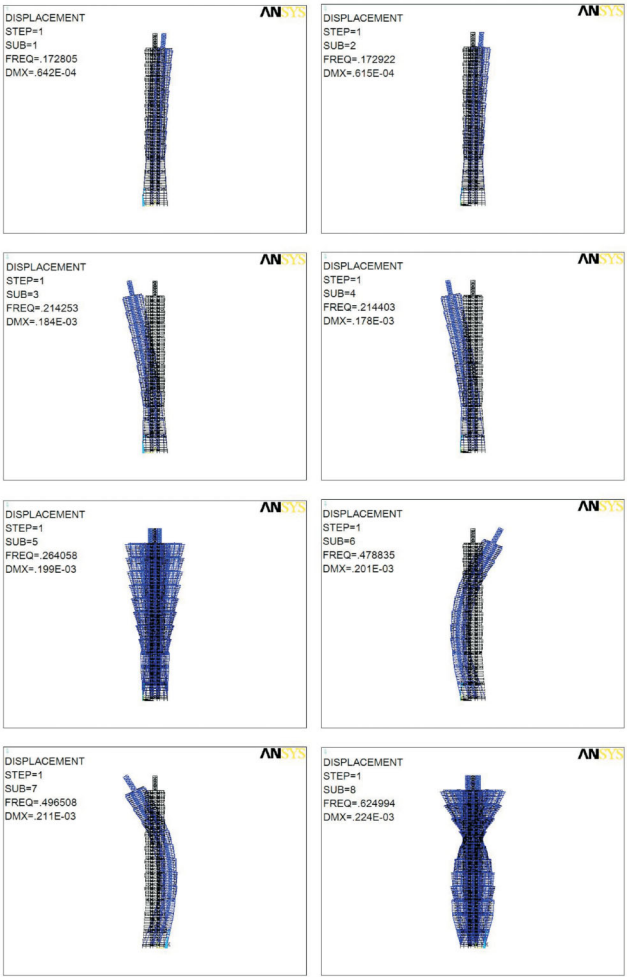

Figure 8. Several mode shapes of Taipei 101 Tower with the TMD.

Table 5. The displacements on the uppermost residential floor, when it is subjected to wind loads

Displacements at the 88th floor (m)	$U_{X\max}$	$U_{Y\max}$	$U_{\theta\max}$
Without-TMD	0.50	1.04	0.0016
With-TMD	0.43	0.76	0.0016
Efficiency of the TMD	14%	27%	--

will stay much longer because the building deflections are effectively reduced.

According to the ISO wind code [22], the total acceleration of the 89th floor is determined using the following formulas:

$$\begin{aligned} a_{x\max} &= \overline{a}_x + g\sigma_{ax} \\ a_{y\max} &= \overline{a}_y + g\sigma_{ay} \\ a_{z\theta\max} &= \overline{a}_{z\theta} + g\sigma_{z\theta} \end{aligned} \tag{28}$$

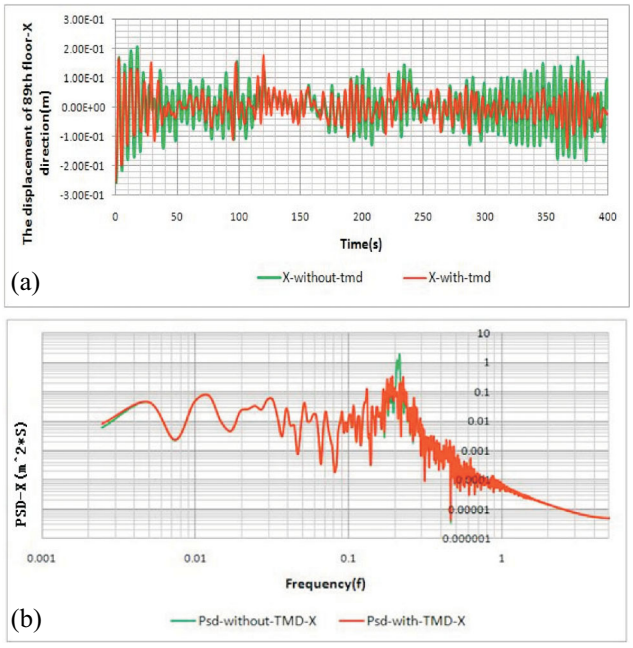

Figure 9. (a) Time history of the along-wind displacement at the top residential floor. (b) Power spectral density of the along-wind displacement at the top residential floor.

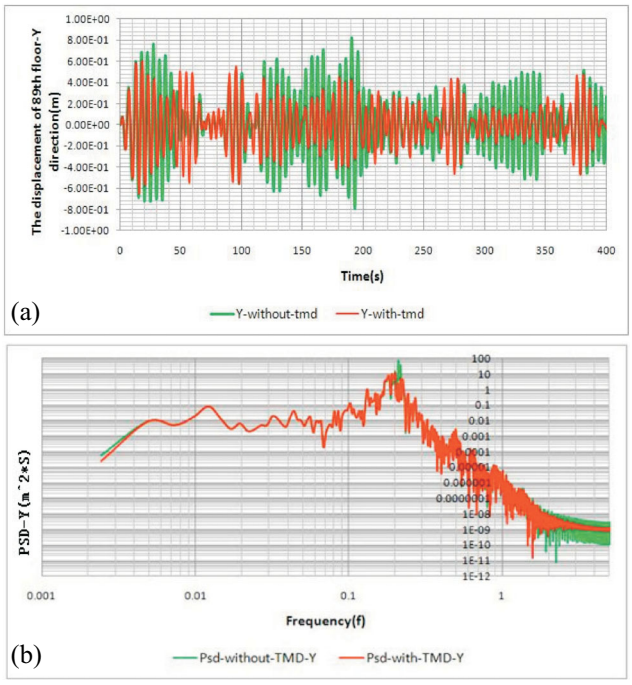

Figure 10. (a) Time history of across-wind displacement at the top residential floor. (b) Power spectral density of across-wind displacement at the top residential floor.

respectively, $a_{x\max}$, $a_{y\max}$, $a_{z\theta\max}$ are the along-wind acceleration, the across-wind acceleration and the rota-

tional acceleration of the uppermost residential floor. The total acceleration of that floor can be expressed as [22]

$$a_{\max} = 0.7\sqrt{{a_{x\max}}^2 + {a_{y\max}}^2 + a_{\theta\max}} \tag{29}$$

The computed accelerations on the uppermost occupied floor, as shown in Table 6, and in Figures 12(a) and 13(a), are largely improved. The resonant response of the first fundamental mode has been modified significantly. As a very encouraging result, the installed TMD system is very effective in mitigating almost all of the undesirable dynamic responses of the building. For example, the across-wind acceleration, which is almost four times the along-wind response, is reduced by 33.7%, and is in good agreement with the 40% reduction recorded in the full-scale measurement [18]. At the same time, the acceleration of the along-wind direction is decreased by 31.7%. Since the TMD is placed at the centroid of the building, no influence is observed in the torsional responses. Similarly, the displacement of the across-wind direction is reduced by 27%, which is better than the 14% reduction in the along-wind direction. Comparing these results with

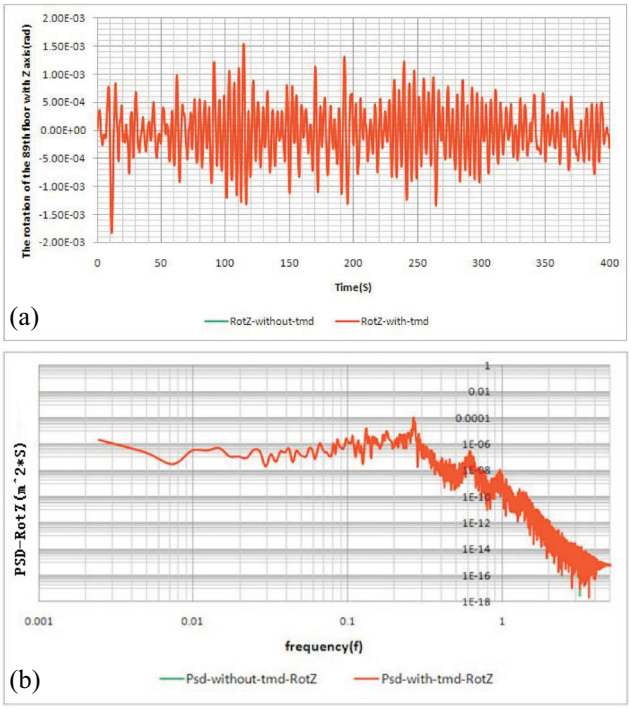

Figure 11. (a) Time history of the rotational displacement at the top residential floor. (b) Power spectral density of rotational displacement at the top residential floor.

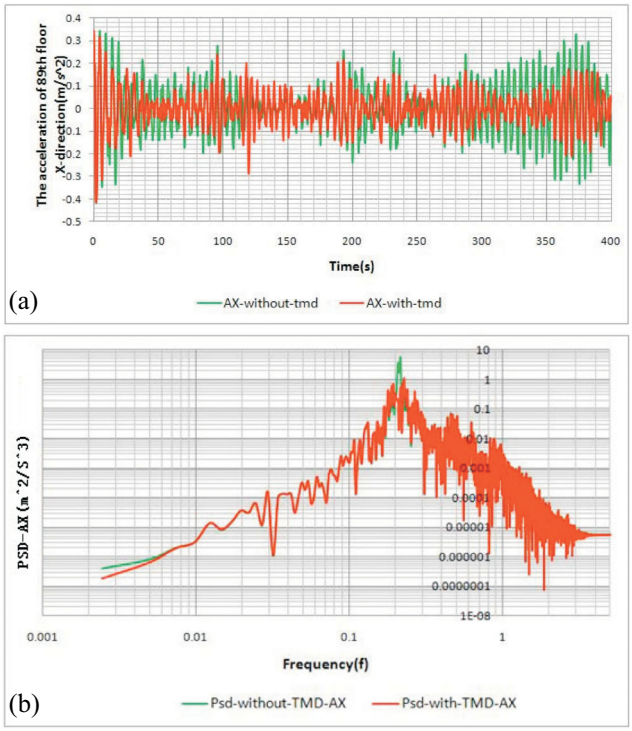

Figure 12. (a) Time history of the along-wind acceleration at the top residential floor. (b) Power spectral density of along-wind acceleration at the top residential floor.

Table 6. The accelerations on the uppermost residential floor, when it is subjected to wind loads

Accelerations of the 88th floor (m^2/s)	$a_{X\max}$	$a_{Y\max}$	$a_{\theta\max}$	$a_{\max}$
Without-TMD	0.39	1.59	0.004	1.15
With-TMD	0.26	1.05	0.004	0.76
Wind tunnel (Without-TMD)		--	--	0.98
Wind tunnel (With-TMD)	--	--	--	0.61
Efficiency	31.7%	33.7%	0	33.6% (FEM) 37.7% (wind tunnel)
Difference (without-TMD)	--	--	--	17.3%
Difference (with-TMD)	--	--	--	24.5%

Note: *difference* = (*FEM* – *wind_tunnel*)/*wind_tunnel*.

the wind tunnel test data [20], Table 6 shows that without TMD, the predicted result for the total acceleration is consistent with the wind tunnel test data, with a difference of 17.3%. It is also shown in Table 6 that there is a relatively large discrepancy, 24.5%, between the computed acceleration and the wind tunnel test result for the structure with TMD. This may be due to the fact that the TMD counted in the wind tunnel test by merely increasing the structural damping ratio from 1.5% to 5%, physically it is not incorporated into the testing model to evaluate its mitigating effect. This could cause different result in the wind tunnel test for the model with the TMD. The frequency domain results presented in Figures 9(b), 10(b), 12(b) and 13(b) suggest that the values of the along-wind responses or across-wind responses at the fundamental modal frequency becomes two peaks while the TMD is installed. The torsional responses (shown in Figures 11 and 14) and the higher modal responses in the along-wind and across-wind direction have not changed. As for the total dynamic response of the building, the fundamental modal responses have the major contribution, which must be controlled (mitigated) to meet the serviceability requirements for comfortable habitation. Conclusively, the installation of the TMD system in this high-rise building is proven to be an effective and economic strategy. Nevertheless, the reduced displacements at the uppermost residential floor also improved the building's long-term performance, the durability of non-structural components, such as the cladding and the vertical shafts for elevators, will be largely improved as well.

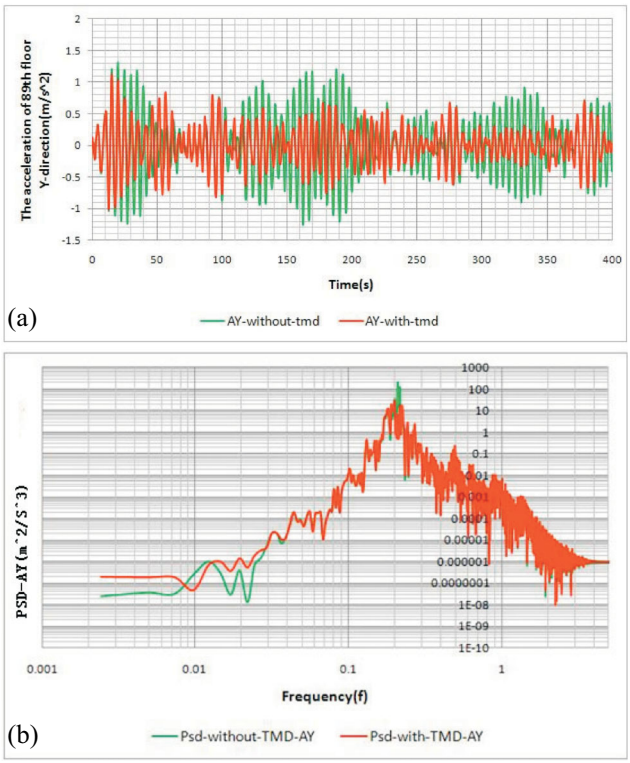

Figure 13. (a) Time history of across-wind acceleration at the top residential floor. (b) Power spectral density of across-wind acceleration at the top residential floor.

8. Remote (Long-distance) Earthquake-Induced Vibration Control Using the TMD System

On May 12, 2008, a devastating tremor, the Wenchuan earthquake, occurred at 02:28 p.m. local time in Sichuan Province of the People's Republic of China, about 1,900 km away from Taipei. The Chinese Earthquake Administration estimated the magnitude of the event as Ms 8.0, with a focal depth of 14 km. A set of acceleration responses from the Taipei 101 Tower during the Wenchuan earthquake were recorded by the monitoring system installed in the building [3], which provided

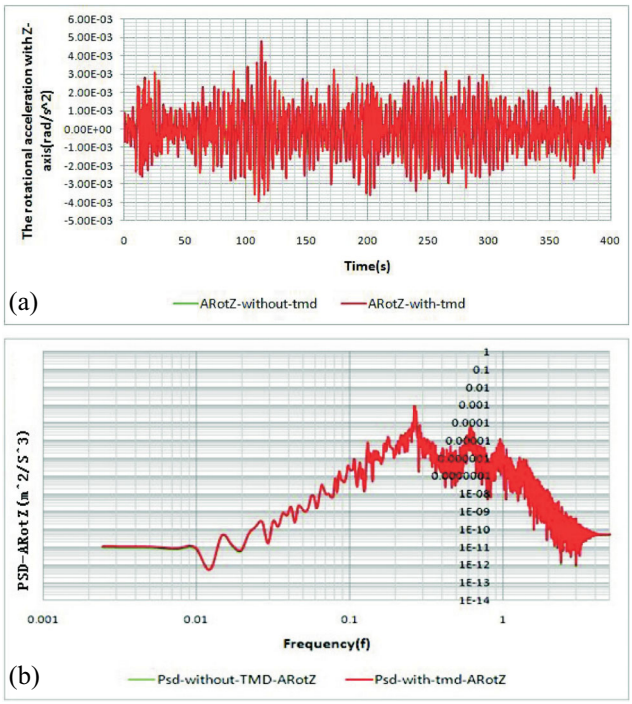

Figure14. (a) Time history of torsional acceleration at the top residential floor. (b) Power spectral density of the torsional acceleration at the top residential floor.

very useful and valuable information for the study of the effect of a remote (long-distance) earthquake on the tall, flexible structure.

The characteristics of this remote earthquake are quite different from those of a typical local earthquake, as demonstrated in the field recorded data in Figures 15 and 16. In particular, when the earthquake wave travels a long distance, the high frequency part of its energy has been filtered out and the energy is more concentrated in the low frequency range.

The remote earthquake-induced responses of the 89th floor of the Taipei 101 Tower are shown in Tables 7–8. It is observed that the displacements are quite small, with the maximum value being just 0.054 m (also shown in Figure 17), which is trivial for the structural design of such an extremely tall building. However, as presented in Figure 19, the acceleration responses are relatively large. This indicates that the slender structure amplifies the acceleration responses while a remote earthquake is subjected to the building. Also released in these tables are that, with the TMD, the accelerations at the uppermost occupied floor (89th floor) are considerably reduced. For example, the TMD system contributes a change in the acceleration responses in the X and Y directions of -3% and 19%, respectively, while the total acceleration is reduced by 13%. Figures 18 and 20 demonstrate that the magnitudes of the spectra near the fundamental fre-

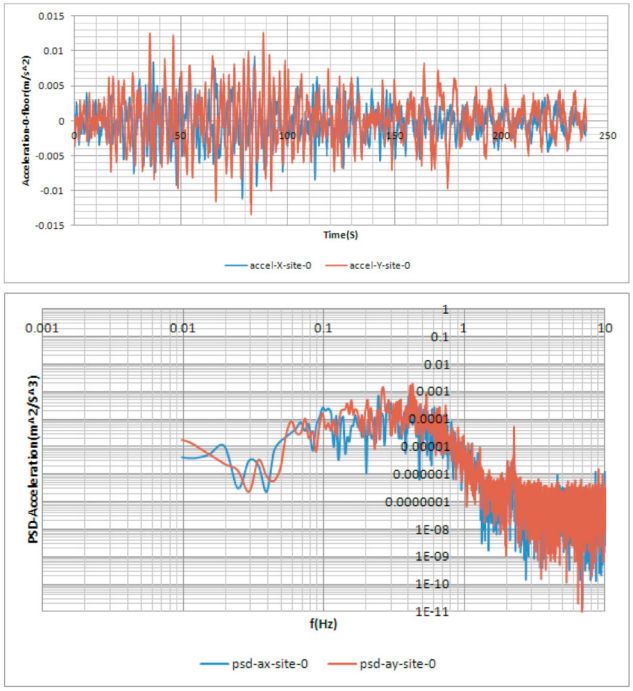

Figure 15. (a) Field measured accelerations at the deepest basement in Taipei 101 Tower. (b) Power spectral density of the field measured accelerations at the deepest basement in Taipei 101 Tower.

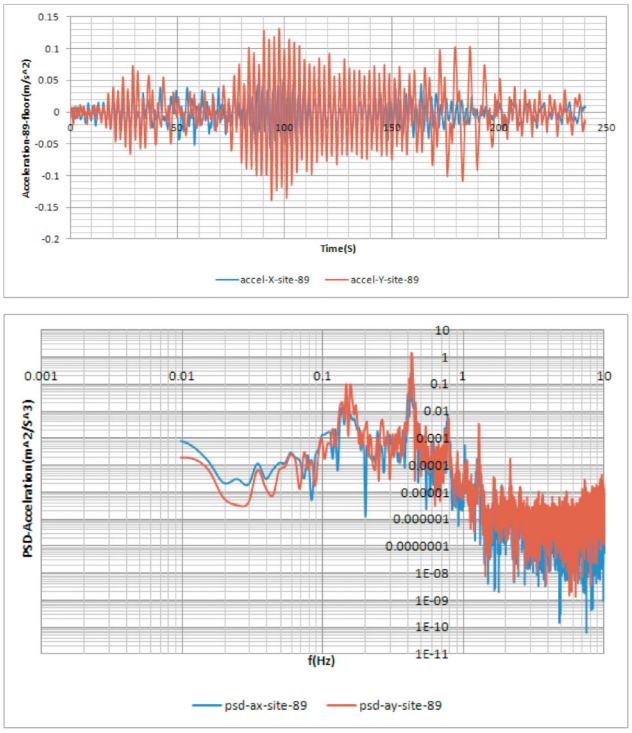

Figure 16. (a) Field measured accelerations at the 89th floor in Taipei 101 Tower. (b) Power spectral density of the accelerations measured at the 89th floor in Taipei 101 Tower.

Table 7. The displacements on the uppermost residential floor, when it is subjected to remote earthquake excitation

Displacements of the 88th floor (m)	$U_{X\max}$	$U_{Y\max}$	$U_{\max}$
Without-TMD	0.027	0.054	0.048
With-TMD	0.020	0.036	0.033
Efficiency	26%	33%	31%

Table 8. The accelerations on the uppermost residential floor, when it is subjected to remote earthquake excitation

Accelerations of the 88th floor (m^2/s)	$a_{X\max}$	$a_{Y\max}$	$a_{\max}$
Without-TMD	0.066	0.109	0.102
With-TMD	0.068	0.089	0089
Field monitored data	0.060	0.140	--
Efficiency	-3%	19%	13%

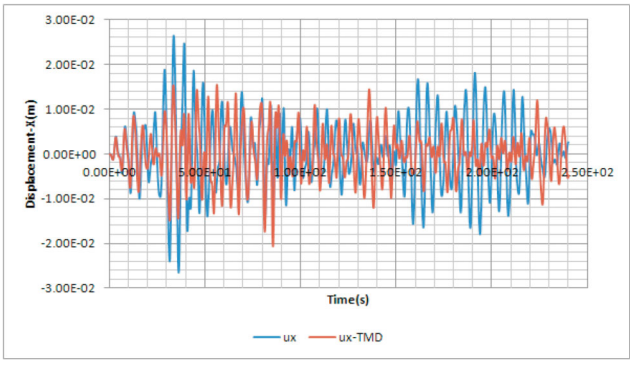

Figure 17. Time histories of the displacements in X direction at the top residential floor for the cases with TMD and without TMD under Wenchuan earthquake excitation.

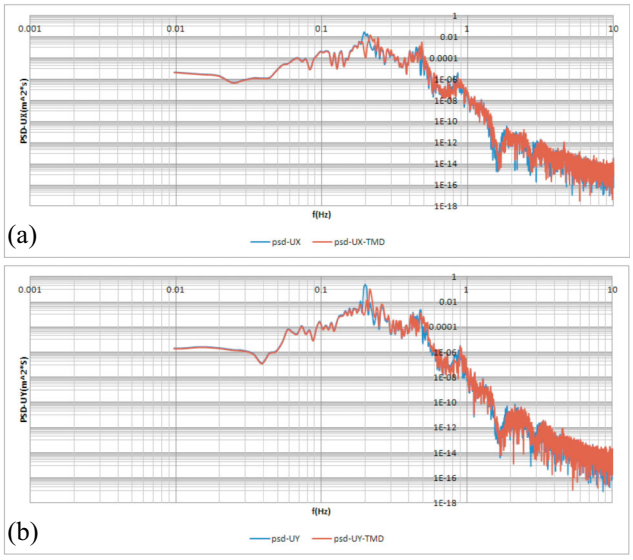

Figure 18. (a) Power spectral density of displacement at the top residential floor. (b) Power spectral density of displacement at the top residential floor.

quency are also reduced. In the higher frequency range, however, the spectral magnitudes have not changed significantly. This situation exposed that, compared with the wind loads, the higher vibration modes of the building are activated by seismic excitation. Since the TMD system can only be tuned up to the first vibration modes of the structure, rather than to the higher vibration modes. Consequently, the mitigation of earthquake-excited vibrations by the TMD is not as effective as its suppression of wind-induced responses.

9. Conclusions

In the analogy of a SDOF system for a MDOF sys-

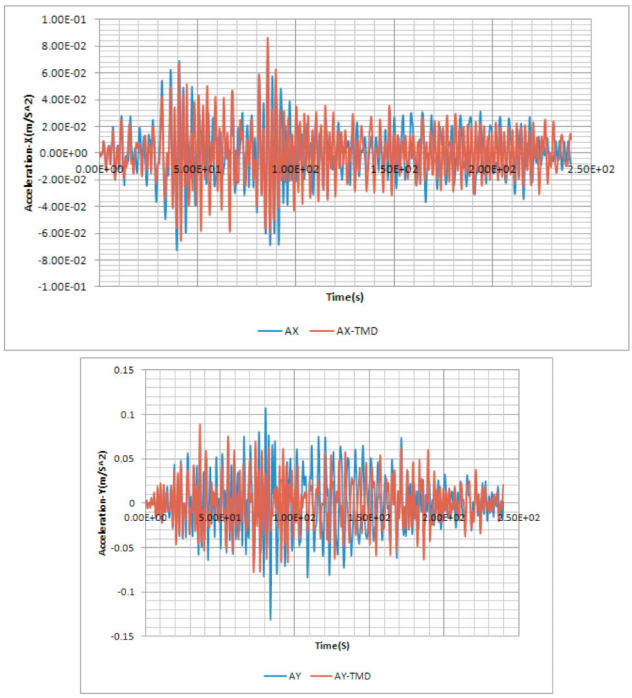

Figure 19. Time histories of accelerations at the top residential floor.

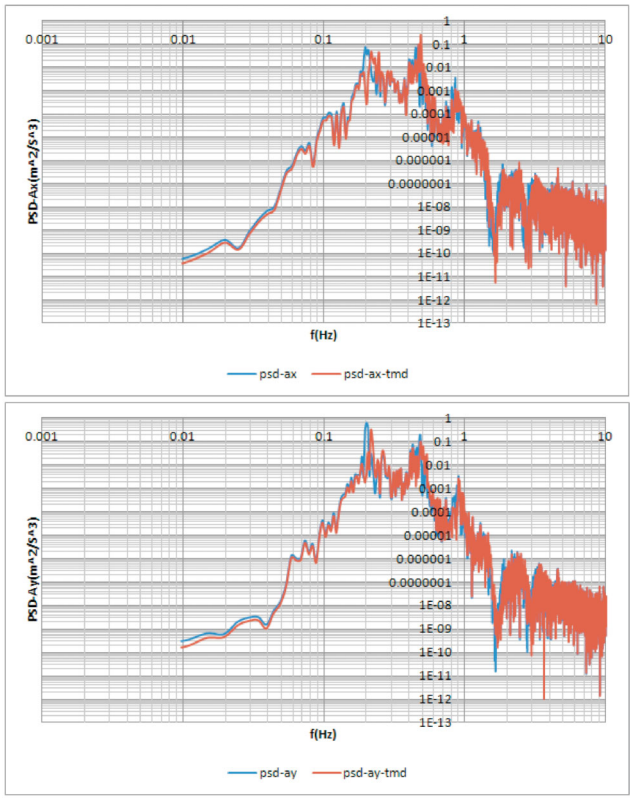

Figure 20. Power spectral density of accelerations at the top residential floor.

tem, both attached with a TMD system, the formulas that used to determine the optimal parameters for a TMD for a MDOF system are derived, to mitigate the dynamic responses of the main system. The developed formulas are then used to evaluate the performance and effectiveness of the 660-ton TMD in the Taipei 101 Tower in mitigating the dynamic vibrations induced by wind loads and a remote earthquake. The objective of this study is to assess the benefits of the TMD in the Taipei 101 Tower, to suggest further development and applications in civil engineering.

The simulation results are found to be in reasonably good agreement with the wind tunnel test data and the full-scale measurements, which verifies the accuracy of the computational framework established in this paper. It is found that after the installation of the TMD, the fundamental mode of the tower has two modes in each direction along the main axis of the building. The modification of the fundamental modes suppresses the wind-induced dynamic responses of the high-rise structure accordingly. The acceleration responses in the along-wind and the across-wind directions are substantially reduced, by 31.7% and 33.8%, respectively. For a remote earthquake event, the total acceleration is reduced by 13%. This is attributed to the fact that as the higher vibration modes of the building are activated by seismic excitation, the effectiveness of the TMD system in decreasing the long-distance earthquake provoked vibrations is not as good as its suppression of wind-induced responses.

Acknowledgements

The authors are very grateful to Dr. Chien-Fu Wu and Dr. Sheng-Chung Su of the National Central Weather Bureau of Taiwan, for their kindly help to provide extensive data recorded at Taipei 101 Tower, in terms of strong winds responses and strong ground motions responses.

The authors also wish to give their special thanks to Chairman Shaw-Sung Hsieh of Evergreen Engineering Consulting Company, the Chief Structural Design Engineer of the Taipei 101 Tower, for his generously provided the valuable information on the structural system designed as well as his precious comments on this study.

This study was partially supported by a grant from the Research Grants Council of the Hong Kong Special Administrative Region, China (Project No: CityU 117 709). The Primary Investigator, Dr. Q. S. Li, is greatly appreciated as well.

References

[1] Pan, T. C., Brownichu, J. M. W. and You, X. T., "Correlating Measured and Simulated Dynamic Response of a Tall Building to Long-Distance Earthquake," *Earthquake Engng Struct. Dyn*., Vol. 33, pp. 611–632 (2004). doi: 10.1002/eqe.366

[2] Brownjohn, J. M. W. and Pan, T. H., "Response of Tall Building to Weak Long Distance Earthquakes," *Earthquake Engng Struct. Dyn*., Vol. 30, pp. 709–729 (2001). doi: 10.1002/eqe.32

[3] Li, Q. S., Zhi, L. H., Tuan, Alex Y., Kao, C. S., Su, S. C. and Wu, C. F., "Dynamic Behavior of Taipei 101 Tower: Field Measurement and Numerical Analysis," *J Struct Eng-ASCE*, Vol. 137, No. 1, pp. 143–155 (2011). doi: 10.1061/(ASCE)ST.1943-541X.0000264

[4] Smith, R., Merello, R. and Willford, M., "Intrinsic and Supplementary Damping in Tall Buildings," Proceedings of the ICE - Structures and Buildings, Vol. 163, No. 2, pp. 111–118 (2010). doi: 10.1680/stbu.2010.163.2.111

[5] Kareem, A. and Kijewski, T., "Mitigation of Motions of Tall Buildings with Specific Examples of Recent Applications," *Wind and Struct*., Vol. 2, No. 3, pp. 201–251 (1999). doi: 10.12989/was.1999.2.3.201

[6] Den Hartog, J. P., *Mechanical Vibrations* (4th edition), McGraw-Hill: New York (1956).

[7] Chang, C. C, "Mass Dampers and Their Optimal Designs for Building Vibration Control," *Eng Struct*., Vol. 21, No. 5, pp. 454–463 (1999). doi: 10.1016/S0141-0296(97)00213-7

[8] Sgobba, S. and Marano, G. C., "Optimum Design of Linear Tuned Mass Dampers for Structures with Nonlinear Behavior," *Mech Syst Signal Processing*, Vol. 24, No. 6, pp. 1739–1755 (2010). doi: 10.1016/j.ymssp.2010.01.009

[9] Leung, A. Y. T. and Zhang, H. J., "Particle Swarm Optimization of Tuned Mass Dampers," *Eng Struct*., Vol. 31, No. 3, pp. 715–728 (2009). doi: 10.1016/j.engstruct.2008.11.017

[10] Leung, A. Y. T., Zhang, H. J., Cheng, C. C. and Lee, Y. Y., "Particle Swarm Optimization of TMD by Non--Stationary Base Excitation during Earthquake," *Earthq Eng & Struct D*, Vol. 37, No. 9, pp. 1223−1246 (2008). doi: 10.1002/eqe.811

[11] Lee, C. L., Chen, Y. T., Chung, L. L. and Wang, Y. P., "Optimal Design Theories and Applications of Tuned Mass Dampers," *Eng Struct*., Vol. 28, No. 1, pp. 43−53 (2006). doi: 10.1016/j.engstruct.2005.06.023

[12] Xu, Y. L., Kwok, K. C. S. and Samali, B., "Control of Wind-Induced Tall Building Vibration by Tuned Mass Dampers," *J Wind Eng Ing Aerodynaimcs*, Vol. 40, No. 1, pp. 1−32 (1992). doi: 10.1016/0167-6105(92)90518-F

[13] Gerges, R. R. and Vickery, B. J., "Wind Tunnel Study of the Across-Wind Response of a Slender Tower with a Nonlinear Tuned Mass Damper," *J Wind Eng Ind Aerod*, Vol. 91, No. 8, pp. 1069−1092 (2003). doi: 10.1016/S0167-6105(03)00053-9

[14] Rana, R. and Soong, T. T., "Parametric Study and Simplified Design of Tuned Mass Dampers," *Eng Struct*., Vol. 20, No. 3, pp. 193−204 (1998). doi: 10.1016/S0141-0296(97)00078-3

[15] Warburton, G. B. and Ayorinde, E. O., "Optimum Absorber Parameters for Simple Systems," *Earthq Eng & Struct Dyn*., Vol. 8, No. 3, pp. 197−217 (1980). doi: 10.1002/eqe.4290080302

[16] Ayorinde, E. O. and Warburton, G. B., "Minimizing Structural Vibrations with Absorbers," *J. Earthq Eng & Struct Dyn*., Vol. 8, No. 3, pp. 219−236 (1980). doi: 10.1002/eqe.4290080303

[17] Warburton, G. B., "Optimum Absorber Parameters for Minimizing Vibration Response," *J Earthq Eng & Struct Dyn*., Vol. 9, No. 3, pp. 251−262 (1981). doi: 10.1002/eqe.4290090306

[18] Research Institute of Building & Construction, Report on the Structural Design Scheme of Taipei 101, Ever Green Consulting Engineering, Inc, Taipei (1999).

[19] Korenev, B. G. and Reznikov, L. M., *Dynamic Vibration Absorbers Theory and Technical Applications*, John Wiley & Sons Ltd (1993).

[20] Wind-Induced Structural Responses Cladding Wind Load Study, Roman Williams Davies & Irwin Inc (RWDI) (1999).

[21] Huang, S. H. and Li, Q. S., "Large Eddy Simulation of Wind Effects on a Supper-Tall Building," *Wind Struct*., Vol. 13, pp. 557−580 (2010). doi: 10.12989/was.2010.13.6.557

[22] International Standards Organization Wind Load Committee, Proposal for Wind Loading Standard, ISO TC 98/SC3/WG2 (1987).

Manuscript Received: Jan. 22, 2014
Accepted: May 23, 2014